

Stimulated Echoes: Description, Applications, Practical Hints

DEBORAH BURSTEIN

*Department of Radiology, DA-705, Beth Israel Hospital, 330 Brookline Avenue, Boston, MA 02215
Phone: 617-667-3349; FAX: 617-667-7021; E-mail: dburstei@bih.harvard.edu*

ABSTRACT

Stimulated echoes are formed from three or more radio frequency pulses. Pulse sequences that use stimulated echoes are extremely versatile because of the availability of three pulses for timing variations and for encoding spatial or chemical shift information. This paper concentrates on the uses of stimulated echoes and on techniques for obtaining them reliably and reproducibly. (Through this understanding, the elimination of undesired stimulated echoes in other pulse sequences should be more straightforward.) Applications include volume-selective spectroscopy; diffusion spectroscopy; and various forms of imaging, such as zoom imaging, chemical-shift-selective imaging, flow imaging, diffusion imaging, multislice imaging, fast imaging, and combinations thereof. © 1996 John Wiley & Sons, Inc.

INTRODUCTION

Stimulated echoes (STEs) are formed from three or more radio frequency (rf) pulses. Pulse sequences that use STEs are extremely versatile because of the availability of three pulses for timing variations and for encoding spatial or chemical shift information. This paper concentrates on their use and on techniques for obtaining them reliably and reproducibly. (Through this understanding, the elimination of undesired STEs in other pulse sequences should be more straightforward.) It will be assumed that the reader has a basic understanding of echoes in general and of basic spectroscopy and imaging pulse sequences.

Received January 23, 1995; revised August 30, 1995; accepted September 29, 1995.

Concepts in Magnetic Resonance, Vol. 8(4) 269-278 (1996)
© 1996 John Wiley & Sons, Inc. CCC 1043-7347/96/040269-10

DESCRIPTION

The timing of the various spin and stimulated echoes that arise from three rf pulses is shown in Fig. 1. The STE arises from spins that refocus because of the combination of all three rf pulses, as described in detail below. However, several other spin echoes are formed from these three rf pulses. Although the formation of these other echoes depends in part on the actual flip angle used for the rf pulses, on relaxation effects, and on the presence of magnetic field gradients, this paper describes the general source of the echoes and their timing so that one might be aware of their occurrence, which can lead to artifacts in the spectra and images.

The first spin echo (SE1) arises from spins that were in the *xy* plane because of the first pulse dephasing and refocusing due to the effects of the

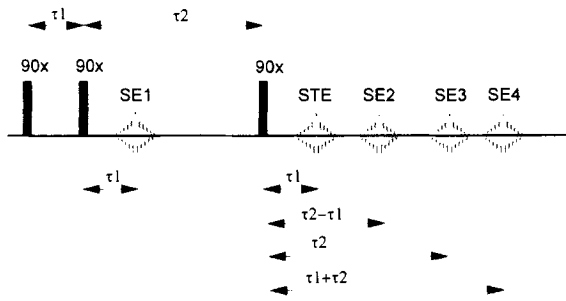


Figure 1 Five echoes arise from the application of three rf pulses. Shown are the timing of the four spin echoes (SE) and the one stimulated echo (STE).

second pulse. Because dephasing time is equal to τ_1 , SE1 forms at a time τ_1 after the second pulse.

After the first spin echo forms, the spins again dephase and can be refocused with the third rf pulse, thus forming the second spin echo. Because the dephasing time here is equal to $\tau_2 - \tau_1$, spin echo 2 (SE2) is formed at a time $\tau_2 - \tau_1$ after the third pulse.

If there were spins in the xy plane immediately after the second rf pulse (dependent on the actual flip angle used and relaxation effects), they could be refocusing by the third pulse. Because the effective dephasing time here is τ_2 , spin echo 3 (SE3) forms at a time τ_2 after the third pulse.

The fourth spin echo is due to spins in the xy plane after the first pulse refocusing with the third pulse (at a time $\tau_1 + \tau_2$ after the third pulse). Note that the actual timing of the various spin echoes depends on the relative magnitude of τ_1 and τ_2 .

Figure 1 brings up the first point regarding the use of pulse sequences with three pulses and the acquisition of the desired stimulated echo:

One must choose the timing and/or conditions of the pulse sequence such that only the echo of interest (the STE, in this case) is refocused within the acquisition period.

One can time out the pulses and acquisition window such that only the STE is within the acquisition window. Alternatively, it is possible to apply magnetic field gradients that will dephase the spin echoes, leaving the STE intact in the acquisition period. This is described below. (It is also possible to separately encode and digitize the various spin and stimulated echoes to obtain different types of information within a single pulse sequence. This application is not discussed in this paper.)

Note that, although the three pulses in Fig. 1 are drawn as part of a single pulse sequence, STEs can arise from a two-pulse pulse sequence with a short repetition (T_R) interval. This is one source

of artifact due to unwanted STEs in fast spin echo pulse sequences; for example, the extra echoes that form during the acquisition period can lead to modulation (banding artifacts) in MR images formed supposedly only from spin echoes.

Formation of the Stimulated Echo

To better explain the behavior of the STE, the spin behavior that leads to its formation is diagrammed in Fig. 2. To give an intuitive description of the general mechanism of STE formation, this description is oversimplified and could in some cases lead to erroneous conclusions if it is used to analyze modifications (such as phase cycling) on the pulse sequence. Therefore, for those who plan to pursue a more rigorous study, a more detailed and accurate description of STEs can be found in the papers cited in the list of general references. The simple diagram of Fig. 2 is useful, however, for presenting a quick and basic framework that can be used to qualitatively explain the issues in pulse sequence design described below.

The first rf pulse (along the x direction in the example shown) creates a y component to the magnetization. We will assume that during the first interval (τ_1) the spins totally dephase in the xy plane ($\tau_1 > 5T_2$), and therefore no net magnetization remains in the xy plane. This can be represented by four equal-sized magnetization vectors along the x , $-x$, y , and $-y$ axes, labeled a, b, c, and d for convenience. Note that a and b have moved by $\pm 90^\circ$ during τ_1 , c has not moved, and d has moved 180° (as seen in the rotating frame). The second 90° pulse (also along x) does not affect the spins along the x direction (a and b); however, it flips the y spins (c) to z and the $-y$ spins (d) to $-z$. (Spins a and b continue to refocus to form

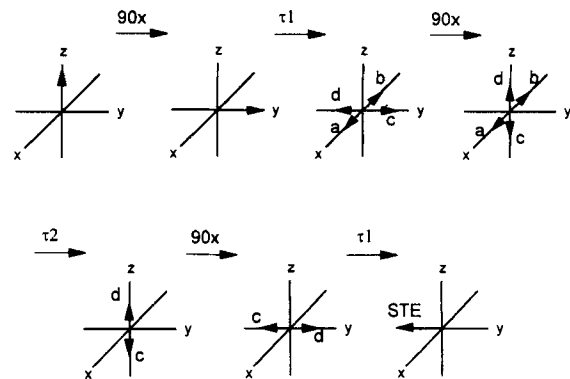


Figure 2 Simplified vector diagram describing the formation of a stimulated echo.

the spin echoes, and will not be considered further here.) The third 90° pulse then flips the magnetization vectors *c* and *d* to $-y$ and $+y$. Because *c* does not move in this rotating frame, and *d* moves 180° during a time τ_1 , *c* and *d* refocus for an STE at a time τ_1 later along the $-y$ axis.

This diagram raises several points:

The spins should be totally dephased in the xy plane, before the second pulse, to obtain a "clean" and maximum intensity STE formation.

The formation of the STE as diagrammed in Fig. 2 relies on dephasing of the spins before the second rf pulse is applied. Therefore, if normal T_2^* mechanisms will not result in dephasing of the spins before the second pulse, a magnetic field gradient can be applied to dephase them; this gradient also must be put in the third interval to reverse the effect of the gradient and refocus the spins. This will be discussed in more detail below.

If the spins are not totally dephased before the second pulse, an STE can still be formed, although it might contain interference from other signals, such as a free-induction decay (FID) off of the third pulse. These interfering signals can be eliminated by phase cycling (requiring more than one acquisition). Note that in the limit of insignificant dephasing between the first two pulses, the sequence is identical to an inversion-recovery pulse sequence (assuming the same phase for the first two pulses) with a resulting FID after the third pulse.

The phase of the spins after the third rf pulse relative to that after the first pulse is comparable to that of a 180° pulse phase change.

This has implications for magnetic field gradient design, described below.

Any rf pulse can be used.

In some situations, a 90° pulse for excitation might not be desirable. For example, low flip angles could be desirable when repeated scans must be acquired for signal averaging and one does not want to wait $5T_1$ as a repetition time. It is left to the reader to convince him/herself that the same basic concepts of Fig. 2 apply even with low-flip-angle pulses.

Stimulated Echo Amplitude

Under the conditions that the spins are totally dephased during the first interval and that diffusion effects are negligible, the amplitude of the STE at a time τ_1 after the third pulse can be written as

$$M = \frac{M_0}{2} \sin(\alpha_1) \sin(\alpha_2) \sin(\alpha_3) e^{-\left[\frac{\tau_2}{T_1} + \frac{2\tau_1}{T_2}\right]} \quad [1]$$

α_1 , α_2 , and α_3 are the phase angles for the three rf pulses. Note that the terminology for the time intervals (τ_1 and τ_2 here) is inconsistent in the literature, and therefore care should be taken when using equations from the literature.

The maximum signal of the stimulated echo is $M_0/2$, half that of the maximum spin echo amplitude.

This results in the often-made comment that "a stimulated echo gives only half the signal to noise as a Hahn spin echo." However, because T_1 effects dominate during the middle interval, in some applications the STE could yield a higher signal-to-noise ratio (S/N) than would a similar experiment run with a spin-echo sequence, such as in the case of the diffusion experiment described below. Similarly, some of the STE's advantages, such as the availability of three pulses for encoding spatial and spectral information, will override the disadvantage of lower S/N in some applications.

The STE will be reduced by T_1 effects during the middle interval and by T_2 effects during the first and third intervals.

All of the spins relax via T_2 mechanisms during the first and third intervals. Vectors *c* and *d* relax by T_1 relaxation during τ_2 . In the extreme case, where τ_2 is long enough that complete T_1 relaxation occurs, a net magnetization vector will be present along $+z$ only when the third rf pulse is given, and obviously no stimulated echo will result. It is left to the reader to convince him or herself that with intermediate time intervals for τ_2 , partial T_1 relaxation occurs that proportionately diminishes STE magnitude.

Basic Pulse Sequence

A basic pulse sequence used to generate an STE is shown in Fig. 3. Note the terminology switch to

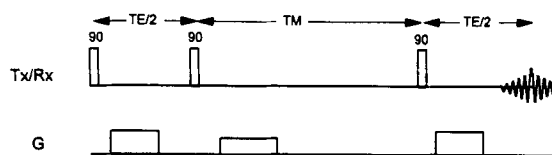


Figure 3 Pulse sequence used to generate a stimulated echo.

$T_E/2$ for the first and third intervals and T_M for the middle interval. The combination of the first and third intervals is referred to as the echo time because this is the time that the spins are in the xy plane.

Magnetic field gradients ("crusher gradients") are used to ensure dephasing of the spins after the first pulse and to eliminate the spin echo formation.

A magnetic field gradient in the first interval is used to ensure dephasing of the spins after the first pulse. This dephasing must be refocused with a magnetic field gradient in the third interval. Note the orientation of the gradient in third interval; it is in the same direction as the first interval because the direction of the spins has been reversed by the rf pulses (see Fig. 2). Although a constant magnetic field gradient (a poor shim) also would be effective in dephasing the spins during $T_E/2$, it also will lead to corresponding effects of magnetic field inhomogeneity in the echo and hence in the spectrum or image.

The magnetic field gradient in the second interval will eliminate the formation of the first spin echo, and hence also the second spin echo. (The first spin echo will form, however, in the specific case where the gradient in the middle interval is put before the time of the formation of the spin echo and matches a gradient that might be present in the first interval.) Similarly, the magnetic field gradient in the third interval will eliminate the formation of the third spin echo, because the spins associated with this echo have not experienced the first magnetic field gradient and therefore will not refocus.

One should check that the signal obtained is really an STE by turning off one rf pulse at a time, and by checking that no significant signal remains.

Several factors can cause an echo that is not a true STE to refocus within the acquisition window, and therefore the signal might not contain the desired information. This could be due to the simple reason of other spin echoes forming within the chosen acquisition window if the magnetic field gradients just described are not used, or it could result from gradient echoes or FIDs off of the third pulse, as will be shown in some examples below. In general, it is always a good idea to test that a true STE is being formed by turning off one rf pulse at a time, and by checking that the signal is lost when any one of the rf pulses is turned off.

Phase cycling can be employed.

Alternatively, one can phase cycle the first pulse and the receiver—as in other standard pulse sequences—to eliminate effects such as receiver off-

sets, undesired signals due to improperly phased pulses, the effects of spins not dephasing totally in the first interval, or extra echoes such as a gradient echo from the third pulse. However, note that phase cycling requires the acquisition and addition–subtraction of at least two acquisitions, and thus it eliminates some of the advantages of the STE pulse sequence, which will be described below.

APPLICATIONS

Volume-Selective Spectroscopy

The pulse sequence for localized spectroscopy by STEs is shown in Fig. 4. Each rf pulse is slice selective along a different axis such that only the spins in a given volume element (voxel) experience all three pulses and will therefore contribute to STE formation. There are two specific characteristics of the pulse sequence to note:

The slice dephasing–refocusing gradients must be in the first or third intervals for all three rf pulses.

Since the spins contributing to the STE are along the z axis in the middle interval, they cannot be dephased or refocused during T_M .

The sequence from the third pulse alone should not simulate a gradient echo pulse sequence unless timing is chosen to avoid acquisition of the gradient echo off of the third pulse.

If the sequence in Fig. 4 is analyzed from the third pulse alone, it appears to be a standard gradient echo pulse sequence. To avoid a gradient echo from the third pulse alone, one could move the third slice-refocusing gradient to the first interval. This has the advantage of eliminating a gradient echo off the third pulse. It also ensures that the spins are dephased in the first interval, as desired for the formation of a pure stimulated echo. The same could be achieved by placing the slice-refocusing gradient from the first or second pulse in

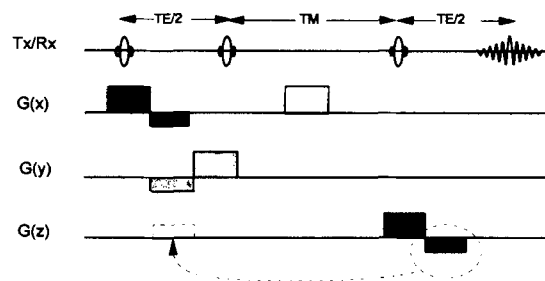


Figure 4 General pulse sequence for volume-selective spectroscopy with stimulated echoes.

the third interval. A drawback of separating the slice-dephasing and slice-rephasing gradients is that, because T_M is usually long, if there is motion of the spins between the first and third pulse (from physiologic motion or diffusion), the distance moved will be greater, and hence the incomplete refocusing of the moving spins will be more severe than it is in spin-echo sequences with the same T_E .

To analyze the resulting signal in spectroscopy mode, it is preferable to digitize (acquire) the signal from the peak of the echo (comparable to the digitization of an FID). However, note that, if the slice-dephasing and slice-rephasing gradients are not trimmed (matched) properly, the peak of the echo will move slightly and the result will be an apparent large first-order phase shift.

There are several advantages to the STE version of localized spectroscopy. First, it is a one-shot technique. Therefore, shimming on the region of interest is simplified, signal acquisition can be very fast if averaging is not required, and there are no subtraction errors such as those that could occur because of motion between acquisitions in localized spectroscopy pulse sequences that rely on the subtraction of two or more acquisitions.

Second, the localized volume is easily imaged with the same basic pulse sequence by including phase encode and readout gradients, as described below in the imaging section.

Finally, the STE results in an echo time half as long as a comparable spin echo formed from a three-pulse localized spectroscopy pulse sequence.

One disadvantage of STE-localized spectroscopy is chemical shift misregistration, which is inherent to any localized spectroscopy technique that uses magnetic field gradients for spatial localization. Because the resonant frequency of the nuclei is used to encode both spatial information and chemical shift (spectral) information, the signal from protons with one chemical shift arises from a volume slightly offset from protons with a different chemical shift.

Diffusion Spectroscopy

One standard technique for measuring diffusion with NMR is the pulsed-gradient-diffusion measurement. The pulse sequence used for measurement of diffusion using STEs is shown in Fig. 5. Briefly, a magnetic field gradient is applied for a short time, δ , during the first $T_E/2$ interval. This imparts a phase to the magnetic moment of each nucleus as a function of its position within the sample. During the second $T_E/2$ interval, a second

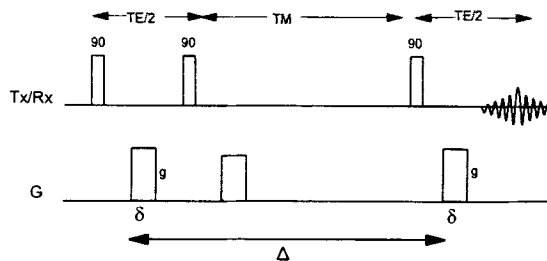


Figure 5 Pulsed gradient diffusion pulse sequence using stimulated echoes.

magnetic field gradient is applied to impart a phase opposite of that of the first gradient, again as a function of position. If the nuclei have not moved, complete refocusing will occur, resulting in a full-amplitude STE.

However, if the nuclei have moved during the time Δ between gradients, the difference between the phase acquired during the first gradient and that acquired during the second gradient—or the net phase change for each magnetic moment—will depend on how far they have moved during Δ . Because of the random motion of the spins in the system, each spin will have acquired a slightly different net phase change because of the two gradients, and there will be a net phase incoherence among magnetic moments within the sample. The resulting STE amplitude will decrease by an amount dependent on the distance the nuclei have moved. Therefore, the amplitude of the STE with the diffusion-sensitizing magnetic field gradients applied is related to the diffusivity of the species under study.

Note that these diffusion effects are present in any pulse sequence that uses gradients in the first and third interval. In general, the magnitude of the gradients used in the first and third intervals for purposes of the STE pulse sequence and the time between gradients (Fig. 3) are small enough such that these diffusion effects are not very significant.

Although either an STE version or a spin echo version (with the pulsed diffusion gradients before and after the 180° pulse) of the pulsed-gradient-diffusion experiment could be used, the STE version has advantages in several specific cases. The first is that in which one is interested in measuring the effective diffusivity (or how far the nuclei have moved) as a function of diffusing time. This would be of interest when the effective distance moved by the spins would depend on how long they are given to diffuse—that is, if the motion at long Δ is limited by structures such as cell membranes.

Because the middle interval (and hence the time between the diffusion gradients) is limited by T_1 relaxation, long diffusion times can be studied. The second situation is that in which species with low diffusivities and short T_2 are under study; if one wants a large effect on the STE amplitude due to diffusion, a long diffusion time can be used by increasing Δ (limited by T_1) with a short T_E . Similarly, if gradient strength is limited and T_2 is short, a stronger diffusion effect can be obtained with a long diffusion time (Δ).

Imaging

The addition of standard slice select, phase encode, and read gradients to the STE pulse sequence enables it to be used for MRI applications (Fig. 6). There are several practical points to be made regarding this sequence, many of which are the same as those described above for localized spectroscopy:

- The gradient reversals for the slice and read gradients need to be within the first and third intervals, because these are the times that the spins of the STE are in the xy plane.
- A crusher gradient can be placed in the middle interval to dephase any spin echoes that might arise in part from the second pulse.
- The read dephasing and phase encode gradients can be placed in the third interval to avoid motion artifacts or extra diffusion weighting.
- The slice reversal for the first pulse also can be placed in the third interval.

If the read and phase encode are in the third interval, moving the first slice-refocusing gradient to the third interval will ensure that the spins de-

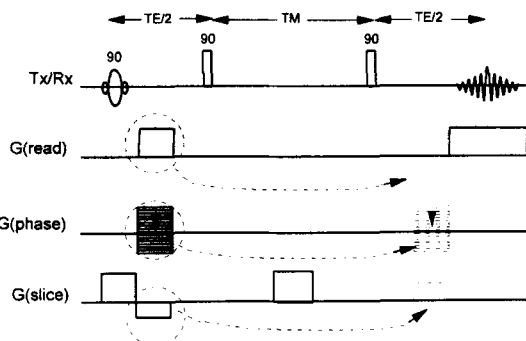


Figure 6 Standard pulse sequence for imaging with the stimulated echo sequence.

phase before the second pulse and that no echo is formed from the third pulse alone. Again, however, one drawback of this approach is decreased refocusing incurred by having a long interval between the slice-rephasing and slice-rephasing gradients if motion is present in the system.

- The slice select gradient can be on any of the three pulses.

Although all three pulses can be made slice selective, just one needs to be to obtain signal from that slice alone (as shown in Fig. 6). Therefore, the availability of three pulses has various applications: chemical-shift-selective imaging, zoom imaging, and flow tagging. In addition, diffusion-sensitizing gradients, such as those described above (Fig. 5), can be used in conjunction with the basic imaging sequence to obtain diffusion-weighted images. These are described below.

Chemical-Shift-Selective Imaging. The pulse sequence for chemical-shift-selective imaging is shown in Fig. 7. The second pulse (in this case) is made frequency selective (“soft”) without a magnetic field gradient on. Therefore, only those spins with chemical shifts of the same frequency as that of the pulse will receive the rf excitation and will contribute to the resulting STE.

Zoom Imaging. The pulse sequence for zoom imaging is shown in Fig. 8. The first two pulses are used to select volumes along two directions; only those spins at the intersection of those volumes will contribute to the STE. The third pulse is then used for imaging of a slice within the selected volume. This is useful for situations in which the sample is larger than the desired field of view. Alternatively, three-dimensional imaging can be done in a three-dimensional zoomed region.

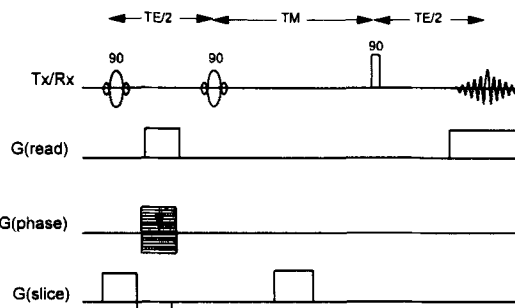


Figure 7 Pulse sequence for chemical-shift-selective imaging with stimulated echoes.

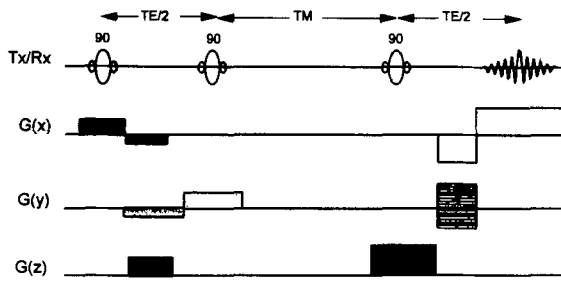


Figure 8 Pulse sequence for zoom imaging with stimulated echoes.

Flow Imaging. The pulse sequence for flow imaging with stimulated echoes is shown in Fig. 9. The first pulse is made slice selective to select a plane of spins. (Alternatively, both the first and second pulses can be made slice selective to select spins at the intersection of two volumes.) The spins are then given time to move during T_M . (Note that the magnetization is in the z direction during this time, reducing dephasing effects.) After the third pulse, an image is obtained with the read gradient in the same direction as the original slice select, thus imaging the bolus of spins that have moved from that plane. With short echo times, dephasing is minimized. For longer echo times, flow-compensated gradients can be used for the read and slice gradients. Note that, if a crusher gradient is used to dephase the spins in the first interval, with a corresponding refocusing gradient in the third interval, it should be in a direction perpendicular to the flow.

Diffusion Imaging. The pulse sequence for imaging of diffusion is shown in Fig. 10. It is essentially the same as the diffusion spectroscopy pulse sequence, with imaging gradients added.

Multislice Imaging. The pulse sequence for multislice imaging is shown in Fig. 11. The read

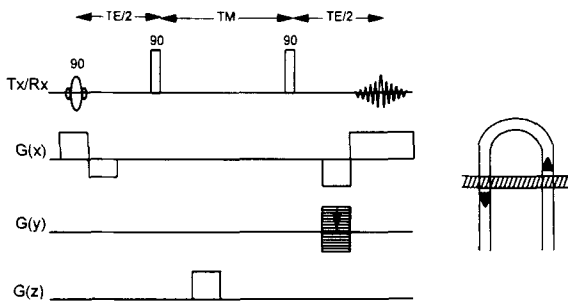


Figure 9 Pulse sequence for flow tag imaging with stimulated echoes.

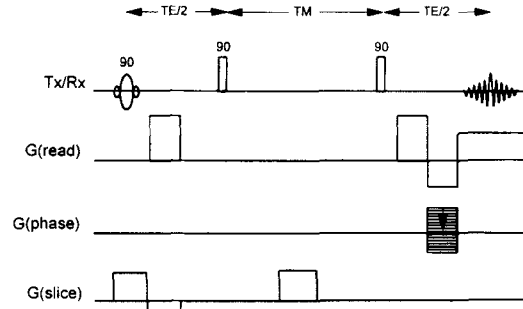


Figure 10 Pulse sequence for diffusion imaging with stimulated echoes.

dephasing and phase encode gradients are placed in the first interval. The third pulse is slice selective, with a standard imaging readout. This third pulse is repeated with different slice select gradients for n different slices. The number of slices is limited by T_1 relaxation (and each will have slightly different T_1 weighting) because T_M will be increased for each successive slice. The entire sequence is repeated for each phase encode step. The read dephasing and phase encode gradients also can be placed in the third interval. This, however, requires higher duty cycles on the gradients.

One large advantage of multislice imaging with STEs as shown is that it can be combined with chemical-shift-selective imaging by making the first pulse chemical shift selective. Thus, just one chemical species in the entire volume, which is then used for multislice encoding, is excited. This is not possible with spin echo imaging, because all of the pulses must be repeated for each slice and therefore the chemical shift (nonspatially selective) pulse would saturate that species.

Combination Sequences. With three pulses available for excitation, the STE pulse sequence is

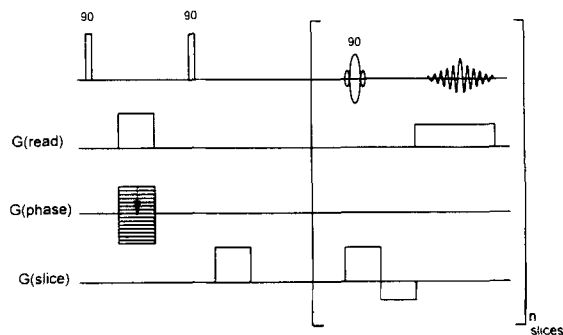


Figure 11 Pulse sequence for multislice imaging with stimulated echoes.

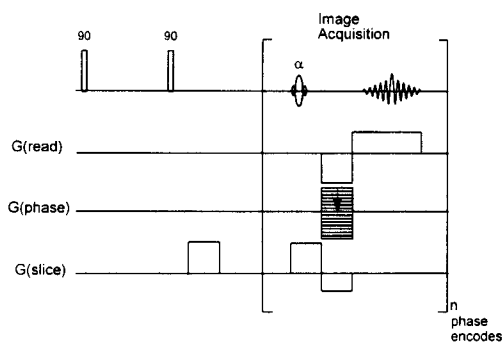


Figure 12 Pulse sequence for fast imaging with stimulated echoes.

versatile. Combinations of the above pulse sequences can be used for specific applications. One (chemical-shift-selective, multislice imaging) has just been described. Another would be the combination of the localized spectroscopy and diffusion experiments of Figs. 4 and 5.

Ultrafast Imaging. In all of the imaging sequences described above, one phase encode step is obtained every time the STE pulse sequence is run. This requires the sequence to be repeated n times for a matrix size of n , with a recycle delay between each sequence. Alternatively, the third pulse can be transmitted as a low-flip-angle pulse, with each rf pulse and readout independent and with a different phase encode gradient value, thus substantially decreasing the time of imaging. The basic pulse sequence is shown in Fig. 12. Again, this ultrafast readout imaging can be combined with the applications described above. However, it must be kept in mind that this fast readout also can generate extra spin or stimulated echoes because of the fast repetition of rf pulses if the gradients do not crush them out.

ACKNOWLEDGMENT

This work was funded in part through grant HL45180 from the National Institutes of Health.

SELECTED BIBLIOGRAPHY

The following materials discuss the formation of stimulated echos in general and their more specific applications.

General References

D. Ballon, M. Garwood, and J. A. Koutcher, "An Analysis of the Intrinsic Resonance Offset Dependence of

Magnetization Generated by Stimulated Echo Pulse Sequences for Noncoupled Spins," *Magn. Reson. Imag.*, **1991**, *9*, 569–575.

J.-M. Fauth, A. Schweiger, L. Braunschweiler, J. Forrer, and R. R. Ernst, "Elimination of Unwanted Echoes and Reduction of Dead Time in Three-Pulse Electron Spin-Echo Spectroscopy," *J. Magn. Reson.*, **1986**, *66*, 74–85.

E. L. Hahn, "Spin Echoes," *Phys. Rev.*, **1950**, *80*, 580–594.

P. B. Kingsley, "Product Operators, Coherence Pathways, and Phase Cycling. Part II. Coherence Pathways in Multipulse Sequences: Spin Echoes, Stimulated Echoes, and Multiple-Quantum Coherences," *Concepts Magn. Reson.*, **1995**, *7*, 115–136.

P. B. Kingsley, "Product Operators, Coherence Pathways, and Phase Cycling. Part III. Phase Cycling," *Concepts Magn. Reson.*, **1995**, *7*, 167–192.

D. E. Woessner, "Effects of Diffusion in Nuclear Magnetic Resonance Spin-Echo Experiments," *J. Chem. Phys.*, **1961**, *34*, 2057–2061.

Applications References

H. Bruhn, J. Frahm, M. L. Gyngell, K.-D. Merboldt, W. Hanicke, and R. Sauter, "Localized Proton NMR Spectroscopy Using Stimulated Echoes: Applications to Human Skeletal Muscle in Vivo," *Magn. Reson. Med.*, **1991**, *17*, 82–94.

D. Burstein, "MR Imaging of Coronary Artery Flow in Isolated and in Vivo Hearts," *JMRI*, **1991**, *1*, 337–346.

A. Caprihan, R. H. Griffey, and E. Fukushima, "Velocity Imaging of Slow Coherent Flows Using Stimulated Echoes," *Magn. Reson. Med.*, **1990**, *15*, 327–333.

C. J. R. Counsell, "Stimulated Echoes and Spin Echoes. Simultaneous Determination of T_2 , Diffusion Coefficient, and rf Homogeneity," *J. Magn. Reson.*, **1993**, *B 101*, 28–34.

A. P. Crawley and R. M. Henkelman, "A Stimulated Echo Artifact from Slice Interference in Magnetic Resonance Imaging," *Med. Phys.*, **1987**, *14*, 842–848.

F. Desmoulin and J. Seeling, "A Homonuclear Shift Correlated and Spatially Localized Spectroscopy Using Stimulated Echoes," *Magn. Reson. Med.*, **1990**, *14*, 160–168.

S. E. Fischer, M. Stuber, M. B. Scheidegger, and P. Boesiger, "Limitations of Stimulated Echo Acquisition Mode (STEAM) Techniques in Cardiac Applications," *Magn. Reson. Med.*, **1995**, *34*, 80–91.

T. K. F. Foo, W. H. Perman, C. S. O. Poon, J. T. Cusma, and J. C. Sandstrom, "Projection Flow Imaging by Bolus Tracking Using Stimulated Echoes," *Magn. Reson. Med.*, **1989**, *9*, 203–218.

E. J. Fordham, S. J. Gibbs, and L. D. Hall, "Partially Restricted Diffusion in a Permeable Sandstone: Observations by Stimulated Echo PFG NMR," *Magn. Reson. Imag.*, **1994**, *12*, 279–284.

J. Frahm, H. Bruhn, M. L. Gyngell, K.-D. Merboldt, W. Hanicke, and R. Sauter, "Localized High-Resolution

- Proton NMR Spectroscopy Using Stimulated Echoes: Initial Applications to Human Brain *in Vivo*," *Magn. Reson. Med.*, **1989**, *9*, 79–93.
- J. Frahm, H. Bruhn, M. L. Gyngell, K-D. Merboldt, W. Hanicke, and R. Sauter, "Localized Proton NMR Spectroscopy in Different Regions of the Human Brain *in Vivo*, Relaxation Times and Concentrations of Cerebral Metabolites," *Magn. Reson. Med.*, **1989**, *11*, 47–63.
- J. Frahm, A. Haase, D. Matthaei, K-D. Merboldt, and W. Hanicke, "Rapid NMR Imaging Using Stimulated Echoes," *J. Magn. Reson.*, **1985**, *65*, 130–135.
- J. Frahm, K-D. Merboldt, and W. Hanicke, "Localized Proton Spectroscopy Using Stimulated Echoes," *J. Magn. Reson.*, **1987**, *72*, 502–508.
- J. Frahm, K-D. Merboldt, W. Hanicke, and A. Haase, "Stimulated Echo Imaging," *J. Magn. Reson.*, **1985**, *64*, 81–93.
- J. Frahm, T. Michaelis, K-D. Merboldt, W. Hanicke, M. L. Gyngell, D. Chien, and H. Bruhn, "Localized NMR Spectroscopy *in Vivo*," *NMR Biomed.*, **1989**, *2*, 188–195.
- F. Franconi and S. Akoka, "Chemical Shift Imaging from Simultaneous Acquisition of a Primary and a Stimulated Echo," *Magn. Reson. Med.*, **1995**, *33*, 683–688.
- F. Franconi, C. B. Sonier, F. Seguin, A. LePape, and S. Akoka, "Acquisition of Spin Echo and Stimulated Echo by a Single Sequence: Application to MRI of Diffusion," *Magn. Reson. Imag.*, **1994**, *12*, 605–611.
- J. Granot, "Selected Volume Excitation Using Stimulated Echoes (VEST). Applications to Spatially Localized Spectroscopy and Imaging," *J. Magn. Reson.*, **1986**, *70*, 488–492.
- A. Haase, J. Frahm, D. Matthaei, W. Hanicke, H. Bomsdorf, D. Kunz, and R. Tischler, "MR Imaging Using Stimulated Echoes (STEAM)," *Radiology*, **1986**, *160*, 787–790.
- H-P. Hafner, E. Radu, and J. Seelig, "Two-Volume Acquisition in Image-Guided Proton Spectroscopy," *Magn. Reson. Med.*, **1990**, *15*, 135–141.
- E. F. Jackson, P. A. Narayana, and D. P. Flamig, "One-Dimensional Spectroscopic Imaging with Stimulated Echoes: Phantom and Human Leg Studies," *Magn. Reson. Imaging*, **1990**, *8*, 153–159.
- E. F. Jackson, P. A. Narayana, and W. A. Kudrle, "A Comparison of Spatially Resolved Spectroscopy and Stimulated Echo Acquisition Mode Sequences for Volume-Localized Spectroscopy," *J. Magn. Reson.*, **1988**, *80*, 23–38.
- W-I. Jung, K. Kuper, F. Schick, M. Bunse, M. Pfeffer, K. Pfeffer, G. Dietze, and O. Lutz, "Localized Phosphorus NMR Spectroscopy: A Comparison of the FID, DRESS, CRISIS/CODEX, and STEAM Methods *in Vitro* and *in Vivo* Using a Surface-Coil," *Magn. Reson. Imag.*, **1992**, *10*, 655–662.
- R. Kimmich and D. Hoepfel, "Volume-Selective Multipulse Spin-Echo Spectroscopy," *J. Magn. Reson.*, **1987**, *72*, 379–384.
- P. B. Kingsley, "Scalar Coupling and Zero-Quantum Coherence Relaxation in STEAM: Implications for Spectral Editing of Lactate," *Magn. Reson. Med.*, **1994**, *31*, 315–319.
- D. Kunz, "Frequency-Modulated Radiofrequency Pulses in Spin-Echo and Stimulated-Echo Experiments," *Magn. Reson. Med.*, **1987**, *4*, 129–136.
- H. Lahrech and A. Briguet, "Proton Spectral Editing in the Inhomogeneous Radiofrequency Field of a Surface Coil Using Modified Stimulated Echoes," *Magn. Reson. Med.*, **1990**, *16*, 342–349.
- H. Lahrech, A. Briguet, D. Graveron-Demilly, E. Hiltbrand, and P. R. Moran, "Modified Stimulated Echo Sequence for Elimination of Signals from Stationary Spins in MRI," *Magn. Reson. Med.*, **1987**, *5*, 196–200.
- H. Lahrech, A. Briguet, and E. Hiltbrand, "Self-Referencing Subtractive Angiography by Modified Stimulated Echo in Magnetic Resonance Imaging," *Phys. Med. Biol.*, **1989**, *34*, 1–4.
- D. Matthaei, J. Frahm, A. Haase, K-D. Merboldt, and W. Hanicke, "Multipurpose NMR Imaging Using Stimulated Echoes," *Magn. Reson. Med.*, **1986**, *3*, 554–561.
- D. Matthaei, A. Haase, J. Frahm, H. Bomsdorf, and W. Vollmann, "Multiple Chemical Shift Selective (CHESS) MR Imaging Using Stimulated Echoes," *Radiology*, **1986**, *160*, 791–794.
- K. D. Merboldt, W. Hanicke, H. Bruhn, M. L. Gyngell, and J. Frahm, "Diffusion Imaging of the Human Brain *in Vivo* Using High-Speed STEAM MRI," *Magn. Reson. Med.*, **1992**, *23*, 179–192.
- K-D. Merboldt, W. Hanicke, and J. Frahm, "Flow NMR Imaging Using Stimulated Echoes," *J. Magn. Reson.*, **1986**, *67*, 336–341.
- K-D. Merboldt, W. Hanicke, and J. Frahm, "Diffusion Imaging Using Stimulated Echoes," *Magn. Reson. Med.*, **1991**, *19*, 233–239.
- P. Mills, W. Chew, L. Litt, and M. Moseley, "Localized Imaging Using Stimulated Echoes," *Magn. Reson. Med.*, **1987**, *5*, 384–389.
- C. T. W. Moonen, M. von Kienlin, P. C. M. van Zijl, J. Cohen, J. Gillen, P. Daly, and G. Wolf, "Comparison of Single-Shot Localization Methods (STEAM and PRESS) for *in Vivo* Proton NMR Spectroscopy," *NMR Biomed.*, **1989**, *2*, 201–208.
- J. W. Pan and R. G. Shulman, "*In Vivo* Human Localized ¹H Spectroscopy," *Magn. Reson. Med.*, **1989**, *12*, 257–258.
- G. S. Payne and M. O. Leach, "On Doubling the Signal in Localised Stimulated Echo Measurements," *Magn. Reson. Imag.*, **1995**, *13*, 629–632.
- T. L. Richards, "¹H NMR Spectroscopic Imaging of the Monkey Brain Using Binomial Water Suppression in a Stimulated-Echo Sequence," *NMR Biomed.*, **1991**, *4*, 187–191.
- W. R. Riddle, S. J. Gibbs, and M. R. Willcott, "Dissecting and Implementing Steam Spectroscopy," *Magn. Reson. Med.*, **1993**, *29*, 378–380.

- W. Sattin, T. H. Mareci, and K. N. Scott, "Exploiting the Stimulated Echo in Nuclear Magnetic Resonance Imaging. I. Method," *J. Magn. Reson.*, **1985**, *64*, 177-182.
- C. H. Sotak, "A Volume-Localized, Two-Dimensional NMR Method for the Determination of Lactate Using Zero-Quantum Coherence Created in a Stimulated Echo Pulse Sequence," *Magn. Reson. Med.*, **1988**, *7*, 364-370.
- C. H. Sotak and J. R. Alger, "A Pitfall Associated with Lactate Detection Using Stimulated-Echo Proton Spectroscopy," *Magn. Reson. Med.*, **1991**, *17*, 533-538.
- C. H. Sotak and D. M. Freeman, "A Method for Volume-Localized Lactate Editing Using Zero-Quantum Coherence Created in a Stimulated-Echo Pulse Sequence," *J. Magn. Reson.*, **1988**, *77*, 382-388.
- C. H. Sotak and L. Li, "MR Imaging of Anisotropic and Restricted Diffusion by Simultaneous Use of Spin and Stimulated Echoes," *Magn. Reson. Med.*, **1992**, *26*, 174-183.
- J. E. Tanner, "Use of the Stimulated Echo in NMR Diffusion Studies," *J. Chem. Phys.*, **1970**, *52*, 2523-2526.
- P. C. M. van Zijl, C. T. W. Moonen, J. R. Alger, J. S. Cohen, and S. A. Chesnick, "High Field Localized Proton Spectroscopy in Small Volumes: Greatly Improved Localization and Shimming Using Shielded Strong Gradients," *Magn. Reson. Med.*, **1989**, *10*, 256-265.
- V. J. Wedeen, R. M. Weisskoff, T. G. Reese, G. M. Beache, B. P. Poncelet, B. R. Rosen, and R. E. Dinsmore, "Motionless Movies of Myocardial Strain-Rates Using Stimulated Echoes," *Magn. Reson. Med.*, **1995**, *33*, 401-408.
- A. H. Wilman and P. S. Allen, "An Analytical and Experimental Evaluation of STEAM versus PRESS for the Observation of the Lactate Doublet," *J. Magn. Reson.*, **1993**, *B 101*, 102-105.
- H. N. Yeung, D. W. Kormos, and D. A. Sebok, "Single-Acquisition Chemical-Shift Imaging of a Binary System with Use of Stimulated Echoes," *Radiology*, **1988**, *167*, 537-540.
- W. Zhang and P. van Hecke, "A Spin-Product-Operator Analysis of the Dephasing Requirement in STEAM-Localized NMR Spectroscopy," *J. Magn. Reson.*, **1991**, *91*, 408-412.
- W. Zhang, D. S. Williams, and C. Ho, "Longitudinal-Spin-Order Filtered STEAM for the Detection of X Nuclei by Volume-Localized ^1H NMR Spectroscopy," *J. Magn. Reson.*, **1991**, *95*, 581-584.



Deborah Burstein received a B.A. in physics from Queens College of the City University of New York and a Ph.D. in medical physics from the Harvard-Massachusetts Institute of Technology Division of Health Sciences and Technology program. She is currently associate professor of radiology at Beth Israel Hospital and Harvard Medical School in Boston. Her main research concerns application of NMR and MRI to cardiovascular and musculoskeletal problems.